UDC 539.3

Z. Yu. Zhuravlova✉

MECHANICAL RESPONSE OF A SEMI-INFINITE POROELASTIC CUBOID TO AN EXTERNAL LOAD

The novelty of the proposed work lies in obtaining an exact analytical solution of the three-dimensional poroelasticity problem for a semi-infinite cuboid. During the solving three-dimensional poroelasticity problems arise mathematical difficulties due to the dimension of the system of differential equations that must be solved. Traditionally, such solutions are mainly obtained with the help of different numerical approaches. The proposed problem is formulated as a three-dimensional boundary value problem in terms of Biot's model, which considers the fully coupled behavior of a homogenized solid phase based on the structural skeleton, and a homogenized fluid phase, describing the interpenetrating fluid. The analytical method of integral transforms is applied to derive the solution. This made it possible to obtain explicit expressions describing the stress in the skeleton and fluid pressure in the pores. The study of these characteristics is carried out depending on various poroelastic properties of the material and types of applied load. The obtained numerical results can be used in engineering simulation of poroelastic structures, as well as an etalon one in the development of new numerical methods for solving problems of three-dimensional poroelasticity.

Key words: *poroelastic semi-infinite cuboid, integral transform, matrix differential calculus, exact solution.*

Poroelasticity models are widely used in engineering, during simulations of behavior of soils and rock masses infiltrated by groundwater, coupling of fluid flow and deformation in biological materials and simulation of diffusion of hydrogen in metals [28]. It explains interest of many authors to the development of new solving methods for poroelasticity problems. Given the small number of works related to the study of poroelastic three-dimensional cuboid bodies using analytical solution methods, the authors considered it useful to indicate many related works using both analytical and numerical methods for solving poroelasticity problems in a three-dimensional formulation.

Finite-difference, finite-element and boundary element methods are most often used methods for numerical solution of the poroelasticity problems. An novel immersed finite element approach is proposed in [26] to treat the mechanical coupling between a deformable porous medium model and an immersed solid model. The development of in silico models to guide the design approach for poroelastic mimics of articular cartilage is done in [32] by implementation of the constitutive models in FEBio, and usage of PDE solver for multiphasic mechanics problems in biological and soft materials. The direct experimental measurement of permeability was conducted in [37] as a function of specimen orientation and strain. A finite element model was developed to identify how various permeability formulations affect compressive response of the tissue simulated by cuboid. Experimental and modeling results suggest the assumption of a constant, isotropic permeability is appropriate. A viscoelastic only model differed considerably from a visco-poroelastic model, suggesting the latter is more appropriate for compressive studies. A comparison of the performance of two finite element solvers for modelling the poroelastic behavior of highly hydrated collagen hydrogels was presented in [14]. Cuboid hydrogel samples were used there. An axisymmetric pressure-velocity finite-difference formulation (PV-FD) based on Biot's poroelastic theory for modeling sound propagation in a homogeneous atmosphere over layered poroelastic ground is presented in [16]. A fast numerical framework for the computation

✉ z.zhuravlova@onu.edu.ua

of acoustic scattering by poroelastic plates of arbitrary geometries is presented in [25]. A boundary element method is applied there to solve the Helmholtz equation subjected to boundary conditions related to structural vibrations. A velocity stress staggered-grid finite difference algorithm for modeling seismic wave propagation in a poroelastic media using Biot's formulation is developed in [11]. The model problems representing a homogeneous media with a single layer sandstone saturated with brine and two-layered homogeneous model are solved there to test this algorithm. The interaction of an incompressible viscous fluid modelled by the dynamic Stokes equation and a multilayered poroelastic structure consisting of a thin linear poroelastic plate layer and a thick Biot layer is considered in [13]. The existence of weak solutions to this fluid-structure interaction problem is proven there using the Rothe method for constructing approximate solutions as well as energy methods and a version of the Aubin – Lions compactness lemma.

Together with pure numerical methods, the use of a mixed (analytically and numerically) approach is quite popular. The dynamic response of an elastic circular plate, under axisymmetric time-harmonic vertical loading, resting on a transversely isotropic poroelastic half-space is investigated in [20] with the use of the discretization techniques and Hankel integral transform. The dynamic response of a rectangular, simply supported, poroelastic plate to a harmonic lateral load is obtained in [33] analytically-numerically for both soil and rock models. The effects of porosities and permeabilities on the response are studied and a comparison between the results for the two material models is made. The quasi-static problem is analysed as a special case of the dynamic one. The Groningen gas field was used in [30] to test a new method to assess stress changes due to gas extraction and forecast induced seismicity. The subsurface is represented as a homogeneous isotropic linear poroelastic halfspace subject to stress changes in three-dimensional space due to reservoir compaction and pore pressure variations. The reservoir is represented by cuboidal strain volumes. Stress changes inside and outside the reservoir are calculated using a convolution with semi-analytical Green functions.

The analytical methods are much less commonly used, especially for the three-dimensional problem statement. Sometimes simplified models are used: it can be or simplification of governing equations of boundary value problem or it can be simplification of geometry such as dimension reduction. The following papers contributed to the development of analytical methods to poroelasticity. A large-strain plate model that allows to describe transient coupled processes involving elasticity and solvent migration was developed in [23] by performing a dimensional reduction of a three-dimensional poroelastic theory. The propagation of Lamb waves in a poroelastic plate containing a linear crack, the special case where the surface of the plate is unloaded, is considered in [18] by employing the Wiener – Hopf technique. Employing Biot's theory, the problem of edge waves in poroelastic plate under plane stress conditions is studied analytically in [27] for both a pervious and an impervious surface. A solution to the problem of water-wave scattering by a semi-infinite submerged thin elastic plate, which is either porous or non-porous, is presented in [31] using the Wiener – Hopf technique. Three-dimensional wave propagation in poroelastic plate immersed in an inviscid elastic fluid is studied analytically in [29] employing Biot's theory. Frequency equations are derived there for pervious and impervious surfaces. The analytical series solution of transient pressure and displacement fields of a finite-size reservoir was developed in [36] using the eigenfunction expansion method. The dynamic displacements of a beam on a poroelastic half space under a periodic oscillating load of constant velocity were analyzed in [19] using Fourier transform. An analytic study of the response of saturated layered half-space under surface point loading was presented in [38], and integral solutions for surface displacements were derived for different hydraulic interface conditions. The general equa-

tions of motion in a homogeneously pre-stressed fluid-saturated medium were formulated in [22], and they were used to derive explicit dependencies of velocity on stresses. Continuum-type mechanics of porous media having a generally anisotropic, product-like fractal geometry was considered in [21], and a new line transformation coefficient was proposed.

The analysis of the existing methods for the determination of physical constants of porous media saturated with liquids was provided in [6] based on static and quasistatic methods of measurements with regard for the initial stresses in the material. The formulation of the mathematical model of thermoelastic solid body taking account of structural heterogeneity of the body material and geometric irregularity of its surface was proposed in [24] with the help of the methods of irreversible thermomechanics and functional analysis.

The thermoelastic and poroelastic problems have similar structures, so some methods used for solving the thermoelastic problems can be applied for the solving of poroelasticity problems. A numerical-analytic method for the determination of one-dimensional static thermoelastic states of plane multilayer structures with arbitrary types of temperature dependences of the physical and mechanical characteristics of the materials of their components was proposed in [7]. A semi-analytical algorithm for solving a three-dimensional thermoelasticity problem for a parallelepiped with free edges was presented in [39]. The direct integration method and apparatus of Vihak key functions were used there. The problem of investigation of the thermal stressed state in a system formed by semitransparent and opaque thermossensitive layers that is caused by the thermal irradiation on the side of the opaque layer was formulated and solved in [3]. The problem of harmonic torsional loading of an infinite elastic composite formed by alternating plane layers made of two different materials in the presence of a penny-shaped crack in one of the components of periodic structure was considered in [10]. Frictionless contact between an elastic body and a rigid base was simulated in [5] in the presence of periodically located recesses of a quasi-elliptical shape. The integral equations of stationary thermal conductivity for a half-space with detected revealed cracks were derived in [4]. The methods of solving two-dimensional boundary value problems for isotropic bodies were considered in [9].

As it can be seen from the review, the analytical solutions of three-dimensional problems for poroelastic cuboids are rarely found, however, three-dimensional objects are the most valuable models for simulation in engineering. In the proposed paper, the author derived an exact solution of the poroelasticity problem for a semi-infinite cuboid.

1. The statement of the problem. The poroelastic semi-infinite cuboid, $0 < X < \infty$, $0 < Y < b$, $0 < Z < c$ (or, in dimensionless form, $0 < x < \infty$, $0 < y < 1$, $0 < z < h$, $h = c/b$) (Fig. 1) is considered within the framework of the Biot model [12].

The face $x = 0$ is loaded

$$\sigma_x^F\big|_{x=0} = -L(y,z), \qquad \tau_{xy}^F\big|_{x=0} = Y(y,z),$$

$$\tau_{xz}^F\big|_{x=0} = Z(y,z), \qquad p|_{x=0} = P(y,z), \quad 0 < y < 1, \quad 0 < z < h, \tag{1}$$

where $p(x,y,z)$ is dimensionless pore pressure, $\sigma_x^F(x,y,z)$, $\tau_{xy}^F(x,y,z)$, $\tau_{xz}^F(x,y,z)$ are dimensionless normal and shear total stresses (the initial characteristics are referred to the shear modulus G).

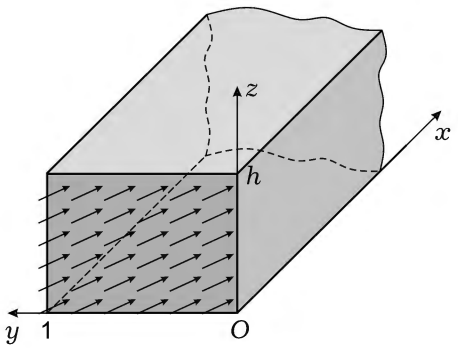

Fig. 1. Geometry and coordinate system of the poroelastic semi-infinite cuboid.

Using the relations between total and effective stresses [35], conditions (1) can be rewritten in the following form

$$\sigma_x\big|_{x=0} = -L(y,z) - \alpha P(y,z), \qquad \tau_{xy}\big|_{x=0} = Y(y,z),$$

$$\tau_{xz}\big|_{x=0} = Z(y,z), \qquad p\big|_{x=0} = P(y,z), \qquad 0 < y < 1, \qquad 0 < z < h, \qquad (2)$$

where $\sigma_x(x,y,z)$, $\tau_{xy}(x,y,z)$, $\tau_{xz}(x,y,z)$ are dimensionless normal and shear effective stresses, α is the Biot coefficient [15].

At the faces $y = 0$, $y = 1$, $z = 0$, $z = h$ the conditions of slide contact with undrained conditions are fulfilled

$$v\big|_{y=0} = 0, \qquad \tau_{xy}\big|_{y=0} = 0, \qquad \tau_{yz}\big|_{y=0} = 0, \qquad \left.\frac{\partial p}{\partial y}\right|_{y=0} = 0, \qquad (3)$$

$$v\big|_{y=1} = 0, \qquad \tau_{xy}\big|_{y=1} = 0, \qquad \tau_{yz}\big|_{y=1} = 0, \qquad \left.\frac{\partial p}{\partial y}\right|_{y=1} = 0, \qquad (4)$$

$$w\big|_{z=0} = 0, \qquad \tau_{xz}\big|_{z=0} = 0, \qquad \tau_{yz}\big|_{z=0} = 0, \qquad \left.\frac{\partial p}{\partial z}\right|_{z=0} = 0, \qquad (5)$$

$$w\big|_{z=h} = 0, \qquad \tau_{xz}\big|_{z=h} = 0, \qquad \tau_{yz}\big|_{z=h} = 0, \qquad \left.\frac{\partial p}{\partial z}\right|_{z=h} = 0. \qquad (6)$$

Here $u(x,y,z)$, $v(x,y,z)$, $w(x,y,z)$ are dimensionless displacements of the solid skeleton (the displacements are referred to the value of b).

The system of equilibrium and storage equations has the following form [35]

$$\frac{\varkappa+1}{\varkappa-1}\frac{\partial^2 u}{\partial x^2} + \frac{\partial^2 u}{\partial y^2} + \frac{\partial^2 u}{\partial z^2} + \frac{2}{\varkappa-1}\left(\frac{\partial^2 v}{\partial x\partial y} + \frac{\partial^2 w}{\partial x\partial z}\right) - \alpha\frac{\partial p}{\partial x} = 0,$$

$$\frac{\partial^2 v}{\partial x^2} + \frac{\varkappa+1}{\varkappa-1}\frac{\partial^2 v}{\partial y^2} + \frac{\partial^2 v}{\partial z^2} + \frac{2}{\varkappa-1}\left(\frac{\partial^2 u}{\partial x\partial y} + \frac{\partial^2 w}{\partial y\partial z}\right) - \alpha\frac{\partial p}{\partial y} = 0,$$

$$\frac{\partial^2 w}{\partial x^2} + \frac{\partial^2 w}{\partial y^2} + \frac{\varkappa+1}{\varkappa-1}\frac{\partial^2 w}{\partial z^2} + \frac{2}{\varkappa-1}\left(\frac{\partial^2 u}{\partial x\partial z} + \frac{\partial^2 v}{\partial y\partial z}\right) - \alpha\frac{\partial p}{\partial z} = 0,$$

$$\frac{\partial^2 p}{\partial x^2} + \frac{\partial^2 p}{\partial y^2} + \frac{\partial^2 p}{\partial z^2} - \frac{\alpha}{K}\left(\frac{\partial u}{\partial x} + \frac{\partial v}{\partial y} + \frac{\partial w}{\partial z}\right) - \frac{S_P}{K}p = 0, \qquad (7)$$

where $\varkappa = 3 - 4\mu$ is Muskhelishvili's constant, μ is the Poisson ratio, G is shear modulus, $K = h^2/(Gk)$, $S_P = S_p G$ are dimensionless values, S_p is the

storativity of the pore space, k is the permeability coefficient [15.

The stresses, pore pressure and displacements inside the semi-infinite cuboid that satisfy relations (2)–(7) should be found.

2. The exact solution of the problem. To reduce the boundary value problem (2)–(7) to one-dimensional problem the finite Fourier sine and cosine transforms with respect to variables z and y are applied by the following schemes [1]:

$$\begin{Bmatrix} u_\gamma(x,y) \\ v_\gamma(x,y) \\ w_\gamma(x,y) \\ p_\gamma(x,y) \end{Bmatrix} = \int_0^h \begin{Bmatrix} u(x,y,z) \\ v(x,y,z) \\ w(x,y,z) \\ p(x,y,z) \end{Bmatrix} \begin{Bmatrix} \cos\gamma z \\ \cos\gamma z \\ \sin\gamma z \\ \cos\gamma z \end{Bmatrix} dz, \qquad \gamma = \gamma_n = \frac{\pi n}{h},\ n = 0,1,2,\dots,$$

$$\begin{Bmatrix} u_{\gamma\beta}(x) \\ v_{\gamma\beta}(x) \\ w_{\gamma\beta}(x) \\ p_{\gamma\beta}(x) \end{Bmatrix} = \int_0^1 \begin{Bmatrix} u_\gamma(x,y) \\ v_\gamma(x,y) \\ w_\gamma(x,y) \\ p_\gamma(x,y) \end{Bmatrix} \begin{Bmatrix} \cos\beta y \\ \sin\beta y \\ \cos\beta y \\ \cos\beta y \end{Bmatrix} dy, \qquad \beta = \beta_k = \pi k,\ k = 0,1,2,\dots.$$

The application of the transforms to the original boundary value problem lead to one-dimensional problem in the transform domain

$$\frac{d^2 v_{\gamma\beta}}{dx^2} - \left(\beta^2 \frac{æ+1}{æ-1} + \gamma^2\right) v_{\gamma\beta} - \frac{2\beta}{æ-1}\left(\frac{du_{\gamma\beta}}{dx} + \gamma w_{\gamma\beta}\right) + \alpha\beta p_{\gamma\beta} = 0,$$

$$\frac{d^2 u_{\gamma\beta}}{dx^2} - (\beta^2 + \gamma^2)\frac{æ-1}{æ+1} u_{\gamma\beta} + \frac{2}{æ+1}\left(\beta \frac{dv_{\gamma\beta}}{dx} + \gamma \frac{dw_{\gamma\beta}}{\partial x}\right) - \alpha \frac{æ-1}{æ+1}\frac{dp_{\gamma\beta}}{dx} = 0,$$

$$\frac{d^2 w_{\gamma\beta}}{dx^2} - \left(\beta^2 + \gamma^2 \frac{æ+1}{æ-1}\right) w_{\gamma\beta} - \frac{2\gamma}{æ-1}\left(\frac{du_{\gamma\beta}}{dx} + \beta v_{\gamma\beta}\right) + \alpha\gamma p_{\gamma\beta} = 0,$$

$$\frac{d^2 p_{\gamma\beta}}{dx^2} - \left(\beta^2 + \gamma^2 + \frac{S_P}{K}\right) p_{\gamma\beta} - \frac{\alpha}{K}\left(\frac{du_{\gamma\beta}}{dx} + \beta v_{\gamma\beta} + \gamma w_{\gamma\beta}\right) = 0$$

$$\left[(æ+1)\frac{du_{\gamma\beta}}{dx} + (3-æ)(\beta v_{\gamma\beta} + \gamma w_{\gamma\beta})\right]\Big|_{x=0} = (æ-1)L_{\gamma\beta},$$

$$\left[\frac{dv_{\gamma\beta}}{dx} - \beta u_{\gamma\beta}\right]\Big|_{x=0} = Y_{\gamma\beta}, \qquad \left[\frac{dw_{\gamma\beta}}{dx} - \gamma u_{\gamma\beta}\right]\Big|_{x=0} = Z_{\gamma\beta}, \qquad p_{\gamma\beta}\big|_{x=0} = P_{\gamma\beta}. \quad (8)$$

The boundary value problem (8) can be rewritten in vector form [34]

$$\mathbf{L}_2 \mathbf{y}_{\gamma\beta}(x) = \mathbf{0}, \qquad 0 < x < \infty,$$

$$\mathbf{A}_{\gamma\beta}\mathbf{y}'_{\gamma\beta}(0) + \mathbf{B}_{\gamma\beta}\mathbf{y}_{\gamma\beta}(0) = \mathbf{g}_{\gamma\beta}. \quad (9)$$

Here $\mathbf{L}_2$ is a differential operator of the second order, $\mathbf{y}_{\gamma\beta}(x)$ is the vector containing displacements and pore pressure transforms, $\mathbf{A}_{\gamma\beta}$, $\mathbf{B}_{\gamma\beta}$ are known matrices and $\mathbf{g}_{\gamma\beta}$ is a known vector. All these expressions are given in ***Appendix A***.

The method of matrix differential calculation [17] is applied to solve the vector boundary value problem (9). According to it, the solution of the corresponding matrix equation should be found

$$\mathbf{L}_2\mathbf{Y}_{\gamma\beta}(x) = \mathbf{0}, \qquad 0 < x < \infty. \tag{10}$$

Here $\mathbf{Y}_{\gamma\beta}(x)$ is a 4×4-matrix. Let us choose the matrix $\mathbf{Y}_{\gamma\beta}(x)$ in the form $\mathbf{Y}_{\gamma\beta}(x) = e^{\xi x}\mathbf{I}$, and substitute it into the equation (10). The equality $\mathbf{L}_2 e^{\xi x}\mathbf{I} = \mathbf{M}_{\gamma\beta}(\xi)e^{\xi x}$ we derive, where

$$\mathbf{M}_{\gamma\beta}(\xi) =$$

$$= \begin{pmatrix} \xi^2 - \left(\beta^2+\gamma^2\right)\frac{æ-1}{æ+1} & \frac{2\beta}{æ+1}\xi & \frac{2\gamma}{æ+1}\xi & -\alpha\xi\frac{æ-1}{æ+1} \\ -\frac{2\beta}{æ-1}\xi & \xi^2 - \left(\beta^2\frac{æ+1}{æ-1}+\gamma^2\right) & -\frac{2\beta\gamma}{æ-1} & \alpha\beta \\ -\frac{2\gamma}{æ-1}\xi & -\frac{2\beta\gamma}{æ-1} & \xi^2 - \left(\beta^2+\gamma^2\frac{æ+1}{æ-1}\right) & \alpha\gamma \\ -\frac{\alpha}{K}\xi & -\frac{\alpha\beta}{K} & -\frac{\alpha\gamma}{K} & \xi^2 - \left(\beta^2+\gamma^2+\frac{S_P}{K}\right) \end{pmatrix}.$$

According to [40], the solution of the matrix homogenous equation is constructed by the formula

$$\mathbf{Y}_{\gamma\beta}(x) = \frac{1}{2\pi i}\oint_C e^{\xi x}\mathbf{M}^{-1}_{\gamma\beta}(\xi)\,d\xi,$$

where $\mathbf{M}^{-1}_{\gamma\beta}(\xi)$ is the inverse matrix to $\mathbf{M}_{\gamma\beta}(\xi)$. The closed contour C covers all singular points of the matrix $\mathbf{M}^{-1}_{\gamma\beta}(\xi)$.

The determinant of the matrix $\mathbf{M}_{\gamma\beta}(\xi)$ has two multiple poles of the third order $\xi = \pm\sqrt{\beta^2+\gamma^2}$ and two simple poles $\xi = \pm\sqrt{\beta^2+\gamma^2+\frac{S_P}{K}+\frac{\alpha^2(æ-1)}{K(æ+1)}}$. With the use of the residual theorem the system of four fundamental matrix solutions $\mathbf{Y}_{\gamma\beta,i}(x)$, $i = 1,\ldots,4$, is derived. The elements of two of these matrices $\mathbf{Y}_{\gamma\beta,1}(x)$, $\mathbf{Y}_{\gamma\beta,3}(x)$ are increasing as $x\to\infty$, whereas elements of the other two matrices $\mathbf{Y}_{\gamma\beta,2}(x)$, $\mathbf{Y}_{\gamma\beta,4}(x)$ are decreasing as $x\to\infty$.

The solution of the boundary value problem (9) for the case when $\beta\neq 0$, $\gamma\neq 0$ has the following form

$$\mathbf{y}_{\gamma\beta}(x) = \left(\mathbf{Y}_{\gamma\beta,2}(x) + \mathbf{Y}_{\gamma\beta,4}(x)\right)\begin{pmatrix} c_1 \\ c_2 \\ c_3 \\ c_4 \end{pmatrix}, \tag{11}$$

where constants c_i, $i = 1,\ldots,4$, are found from the boundary conditions in (9).

Here it is necessary to consider three subcases of the values of β and γ. These partial cases when $\beta = 0$, $\gamma\neq 0$ (***Appendix B***), $\beta\neq 0$, $\gamma = 0$ (***Appendix C***) and $\beta = 0$, $\gamma = 0$ (***Appendix D***) are considered separately, since for these cases the dimensions of fundamental matrices $\mathbf{Y}_{\gamma\beta,2}(x)$, $\mathbf{Y}_{\gamma\beta,4}(x)$ are varied.

The exact solution of the boundary value problem in transform domain is found in explicit form (11). The explicit solutions of subcases are given in ***Appendices*** **(B.2)**, **(C.2)**, **(D.2)**. The analytical solution of the original problem can be derived by the application of the corresponding inverse formulae to these expressions

$$\begin{Bmatrix} u(x,y,z) \\ v(x,y,z) \\ w(x,y,z) \\ p(x,y,z) \end{Bmatrix} = \begin{Bmatrix} u_{00}(x) \\ v_{00}(x) \\ w_{00}(x) \\ p_{00}(x) \end{Bmatrix} + \frac{2}{h}\sum_{n=1}^{\infty} \begin{Bmatrix} u_{\gamma_n,0}(x) \\ v_{\gamma_n,0}(x) \\ w_{\gamma_n,0}(x) \\ p_{\gamma_n,0}(x) \end{Bmatrix} \begin{Bmatrix} \cos\gamma_n z \\ \cos\gamma_n z \\ \sin\gamma_n z \\ \cos\gamma_n z \end{Bmatrix} +$$

$$+ 2\sum_{k=1}^{\infty} \begin{Bmatrix} u_{0,\beta_k}(x) \\ v_{0,\beta_k}(x) \\ w_{0,\beta_k}(x) \\ p_{0,\beta_k}(x) \end{Bmatrix} \begin{Bmatrix} \cos\beta_k y \\ \sin\beta_k y \\ \cos\beta_k y \\ \cos\beta_k y \end{Bmatrix} +$$

$$+ \frac{4}{h}\sum_{n=1}^{\infty}\sum_{k=1}^{\infty} \begin{Bmatrix} u_{\gamma_n,\beta_k}(x) \\ v_{\gamma_n,\beta_k}(x) \\ w_{\gamma_n,\beta_k}(x) \\ p_{\gamma_n,\beta_k}(x) \end{Bmatrix} \begin{Bmatrix} \cos\beta_k y \\ \sin\beta_k y \\ \cos\beta_k y \\ \cos\beta_k y \end{Bmatrix} \begin{Bmatrix} \cos\gamma_n z \\ \cos\gamma_n z \\ \sin\gamma_n z \\ \cos\gamma_n z \end{Bmatrix},$$

$$\beta_k = \pi k, \qquad \gamma_n = \frac{\pi n}{h}.$$

Here $v_{00}(x)$, $w_{00}(x)$, $v_{\gamma_n,0}(x)$, $w_{0,\beta_k} \equiv 0$.

3. The subcases of the problem statement. The proposed solving method enables to solve two other problems which are subcases of the original problem: ***1***) as x and y tend to infinity, a cuboid is converted to a quarter of a layer (Fig. 2); ***2***) as x, y and z tend to infinity, a cuboid is converted to a quarter-space.

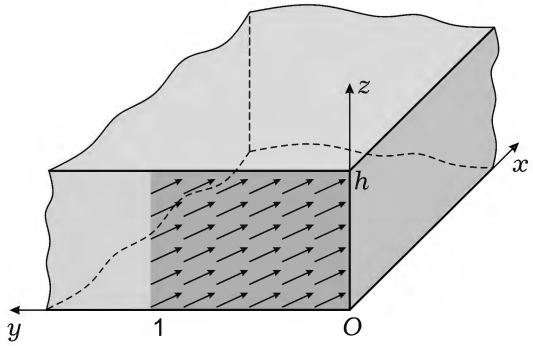

Fig. 2. Geometry and coordinate system of the poroelastic quarter-layer.

The poroelastic quarter-layer is described by the relations $0 < x < \infty$, $0 < y < \infty$, $0 < z < h$, $h = c/b$ (Fig. 2). The boundary conditions (3), (5), (6) are remained the same, but conditions (4) are omitted because of decreasing of all functions on infinity. The loadings in formulas (1) and (2) are supposed to be different from zero only when $0 < y < 1$, $0 < z < h$.

The stress, pore pressure and displacements inside the area that satisfy relations (2), (3), (5)–(7) can be found by the previous scheme. The difference here is that instead of the finite Fourier sine and cosine transform with respect to the variable y the semi-infinite Fourier sine and cosine transform is used. The following solving scheme is saved according to the general case mentioned above. The analytical solution for this problem can be derived by the application of the following inverse formulae

$$\begin{Bmatrix} u(x,y,z) \\ v(x,y,z) \\ w(x,y,z) \\ p(x,y,z) \end{Bmatrix} = \frac{2}{h}\sum_{n=1}^{\infty} \begin{Bmatrix} u_{\gamma_n,0}(x) \\ v_{\gamma_n,0}(x) \\ w_{\gamma_n,0}(x) \\ p_{\gamma_n,0}(x) \end{Bmatrix} \begin{Bmatrix} \cos\gamma_n z \\ \cos\gamma_n z \\ \sin\gamma_n z \\ \cos\gamma_n z \end{Bmatrix} +$$

$$+ \frac{4}{\pi h}\sum_{n=1}^{\infty}\int_0^{\infty} \begin{Bmatrix} u_{\gamma_n,\beta}(x) \\ v_{\gamma_n,\beta}(x) \\ w_{\gamma_n,\beta}(x) \\ p_{\gamma_n,\beta}(x) \end{Bmatrix} \begin{Bmatrix} \cos\beta y \\ \sin\beta y \\ \cos\beta y \\ \cos\beta y \end{Bmatrix} d\beta \begin{Bmatrix} \cos\gamma_n z \\ \cos\gamma_n z \\ \sin\gamma_n z \\ \cos\gamma_n z \end{Bmatrix}, \qquad \gamma_n = \frac{\pi n}{h}.$$

For the poroelastic quarter-space the boundary conditions (3), (5) are the same. The semi-infinite Fourier sine and cosine transforms with respect to variables y and z are used to reduce the stated problem to one-dimensional one. Otherwise, the solving method is the same as described above.

4. Numerical results, discussion and conclusions. The investigation of effective stress and pore pressure was carried out for the semi-infinite parallelepiped and its two partial cases. Two different types of load were considered:

- concentrated normal mechanical load $L(y,z) = \delta(y - 1/2, z - h/2)$, $Y(y,z) = 0$, $Z(y,z) = 0$, $P(y,z) = 0$, where $\delta(y,z)$ is two-dimensional Dirac delta-function;
- distributed normal mechanical load $L(y,z) = -\exp\left(-\left(y-\frac{1}{2}\right)^2 - \left(\frac{z-h/2}{h}\right)^2\right)$, $Y(y,z) = 0$, $Z(y,z) = 0$, $P(y,z) = 0$.

As poroelastic material, there were chosen three different poroelastic materials [15]. Their characteristics are presented in the Table 1, and were used in the dimensionless form for numerical calculations.

Table 1. The characteristics of poroelastic materials [15].

Material \ Properties		$G \cdot 10^{-10}$ [N/m^2]	μ	α	$k \cdot 10^{13}$ [m^4/(N · s)]	$S_p \cdot 10^{11}$ [m^2/N]
1	Charcoal granite	1.87	0.27	0.242	0.001	1.377
2	Westerly granite	1.5	0.25	0.449	0.004	1.412
3	Ruhr sandstone	1.33	0.12	0.637	2.0	2.604

All figures below show the values of normal stresses σ_x, σ_y, σ_z and pore pressure p. The stresses and pore pressure are investigated in the segment $x = a/2$, $z = h/2$, $0 < y < 1$ and influence of different poroelastic materials has been taken into account.

Fig. 3 and Fig. 4 present the case of concentrated normal mechanical load. It can be noted that the maximum absolute values of normal stress and pore pressure are observed at the point $y = 1/2$, $z = h/2$, where the load is applied. The values of normal stress and pore pressure at the boundaries $y = 0$, $y = 1$ are equal. For this case, the stretching stresses σ_x, σ_z at the boundaries $y = 0$, $y = 1$ are observed only close to the boundaries $z = 0$, $z = h$. The stress σ_y is stretching close to the point $y = 1/2$. The largest absolute values at the boundaries $y = 0$, $y = 1$ are seen for σ_x and σ_y. Tangential stresses

are less than normal stresses. Pore pressure at the boundaries $y = 0$, $y = 1$ is negative, which is explained by the impermeable conditions at these boundaries. The similar situation is observed at the lines $z = 0$, $z = h/2$, $z = h$.

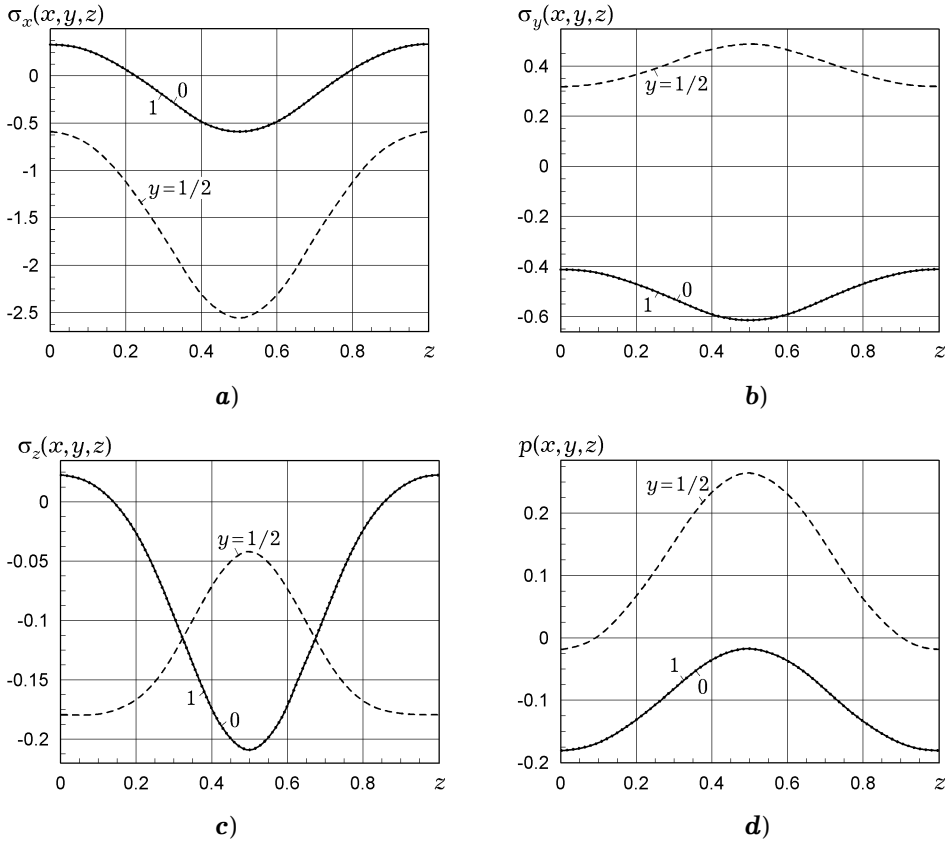

Fig. 3. The distributions of dimensionless effective stress and pore pressure inside the semi-infinite cuboid (Ruhr sandstone) for a concentrated normal mechanical load.

The change of normal stress and pore pressure regarding the change of poroelastic material is shown in Fig. 4. The maximum absolute values of normal stress σ_x, σ_z are observed for the material with the smallest Biot coefficient, while the maximum values of normal stress σ_y and pore pressure are observed for the material with the largest Biot's coefficient. The numbers of curves in all the figures correspond to the numbering of materials in Table 1.

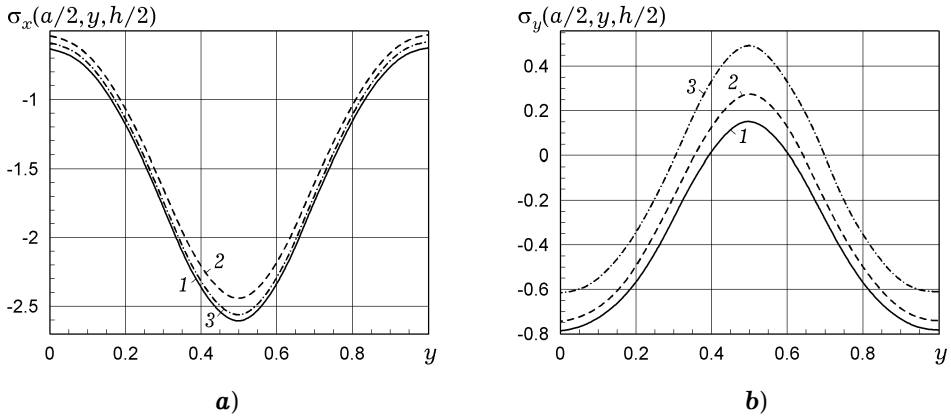

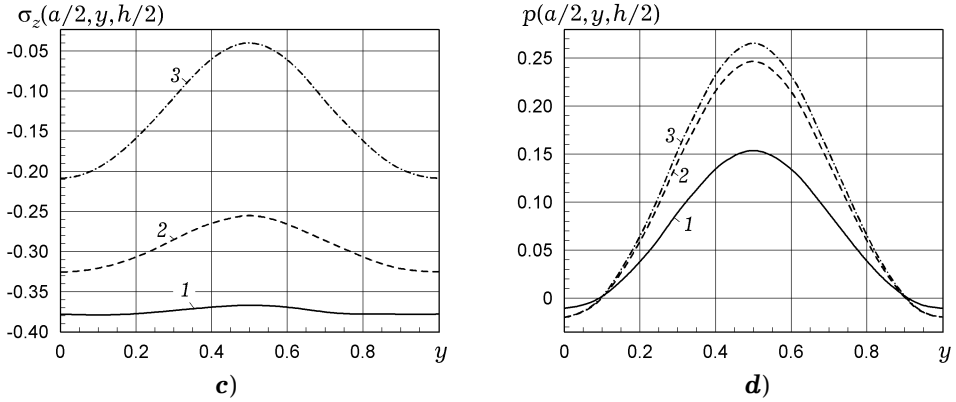

c) ***d***)

Fig. 4. The distributions of dimensionless effective stress and pore pressure inside the semi-infinite cuboid regarding the change of the poroelastic material for a concentrated normal mechanical load.

The case of distributed normal mechanical load is shown in Fig. 5 and Fig. 6. No stretching stress is observed in this case. The largest absolute values at the boundaries $y = 0$, $y = 1$ are seen for σ_x.

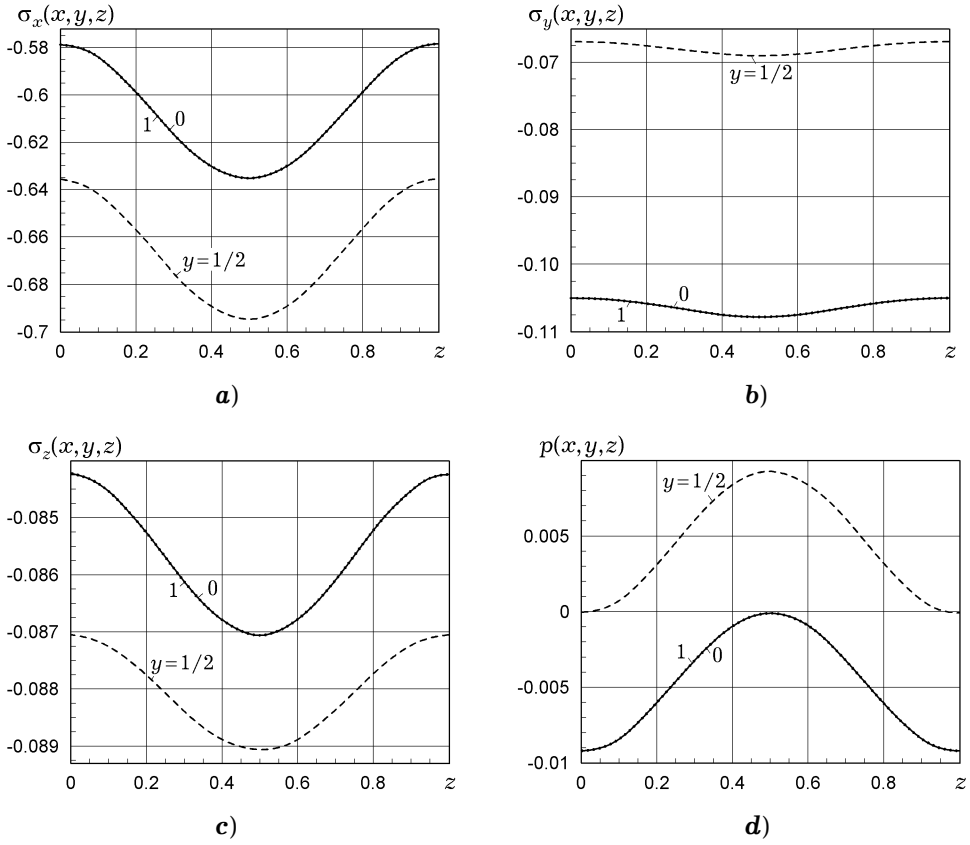

a) ***b***)

c) ***d***)

Fig. 5. The distributions of dimensionless effective stress and pore pressure inside the semi-infinite cuboid (Ruhr sandstone) for a distributed normal mechanical load.

The investigation of normal stress and pore pressure regarding the poroelastic material is shown in Fig. 6. The largest absolute values of normal stress are observed for the material with the smallest Biot's coefficient, while the largest values of pore pressure are observed for the material with the largest Biot's coefficient.

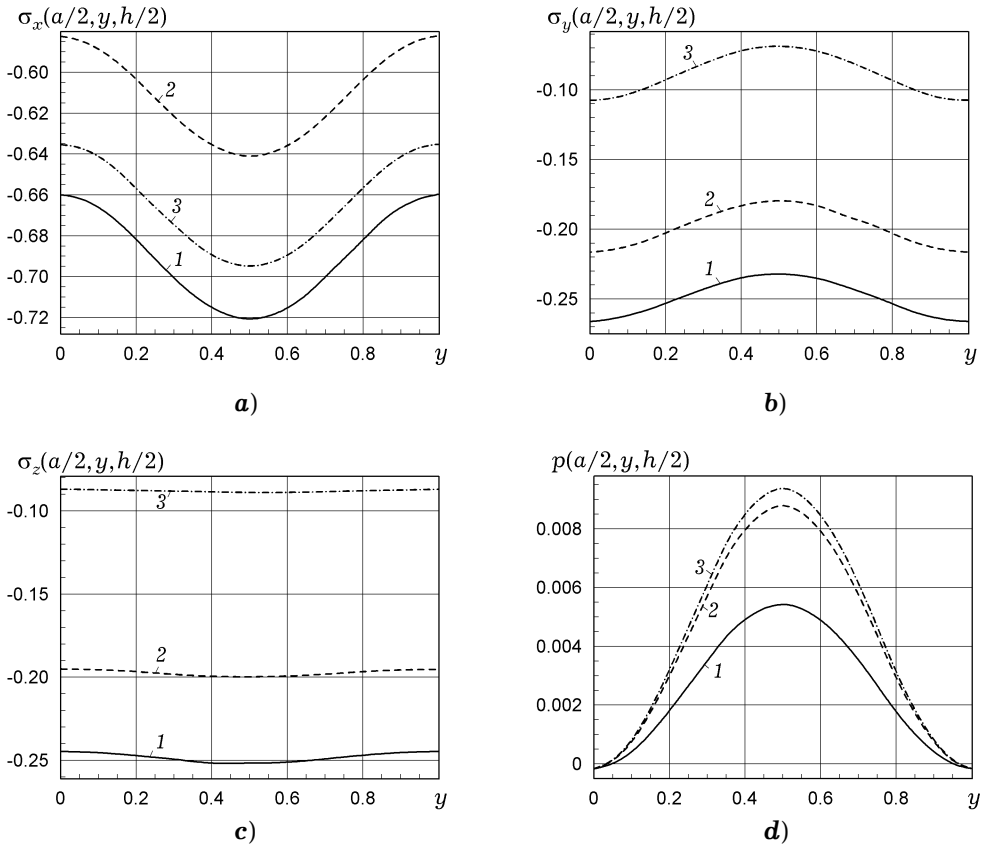

Fig. 6. The distributions of dimensionless effective stress and pore pressure inside the semi-infinite cuboid regarding the change of the poroelastic material for a distributed normal mechanical load.

The obtained results for the subcases were verified when $\alpha = 0$, when they completely coincide with the ones of the elasticity problems for a quarter-space [2] under the same mechanical conditions.

Numerical analysis shows that the largest values of pore pressure are characteristic of the material with the largest Biot's coefficient for all types of applied loading. Tangential stresses are less than normal stress on the faces. The stretching stress is observed only in the case of concentrated normal mechanical load, which means that the statement of the problem should be reformulated for this case, and conditions of perfect contact should be changed. The largest absolute values of normal stress and pore pressure are observed in the case of concentrated normal mechanical load, and the smallest absolute values are observed in the case of distributed fluid pressure load.

The analytical solution for the semi-infinite poroelastic cuboid is derived in the explicit form with the help of integral transform method and apparatus of matrix differential calculation [8]. The modification of the problem statement leads to the solutions of two other problems for the poroelastic quarter-layer and the poroelastic quarter-space. The proposed solving method allows to solve more complex problems in case of changing boundary conditions on the cuboid faces. This complication will make it impossible to obtain the exact solution and will lead to the need to solve singular integral equations. The mentioned problems can be also considered in the case when a defect in the form of a crack or a rigid inclusion is present in the cuboid domain.

Acknowledgments. The research is supported by European project EffectFact No. 101008140 "Effective Factorisation techniques for matrix-functions: Developing theory, numerical methods and impactful applications" funded by the Horizon 2020 Framework Programme for Research and Innovation (2014–2020) (H2020-MSCA-RISE-2020). Scholarship of the Cabinet of Ministers of Ukraine.

Appendix A. The form of matrices and vectors in boundary value vector problem (9) ***in the general case.***

The matrices and vectors shown in (6) have the following forms:

$$\mathbf{L}_2\mathbf{y}_{\gamma\beta}(x) = \mathbf{I}\mathbf{y}''_{\gamma\beta}(x) + \mathbf{Q}_{\gamma\beta}\mathbf{y}'_{\gamma\beta}(x) + \mathbf{O}_{\gamma\beta}\mathbf{y}_{\gamma\beta}(x),$$

$$\mathbf{y}_{\gamma\beta}(x) = \begin{pmatrix} u_{\gamma\beta}(x) \\ v_{\gamma\beta}(x) \\ w_{\gamma\beta}(x) \\ p_{\gamma\beta}(x) \end{pmatrix},$$

$$\mathbf{Q}_{\gamma\beta} = \begin{pmatrix} 0 & \dfrac{2\beta}{æ+1} & \dfrac{2\gamma}{æ+1} & -\alpha\dfrac{æ-1}{æ+1} \\ -\dfrac{2\beta}{æ-1} & 0 & 0 & 0 \\ -\dfrac{2\gamma}{æ-1} & 0 & 0 & 0 \\ -\dfrac{\alpha}{K} & 0 & 0 & 0 \end{pmatrix},$$

$$\mathbf{O}_{\gamma\beta} = \begin{pmatrix} -(\beta^2+\gamma^2)\dfrac{æ-1}{æ+1} & 0 & 0 & 0 \\ 0 & -\left(\beta^2\dfrac{æ+1}{æ-1}+\gamma^2\right) & -\dfrac{2\beta\gamma}{æ-1} & \alpha\beta \\ 0 & -\dfrac{2\beta\gamma}{æ-1} & -\left(\beta^2+\gamma^2\dfrac{æ+1}{æ-1}\right) & \alpha\gamma \\ 0 & -\dfrac{\alpha\beta}{K} & -\dfrac{\alpha\gamma}{K} & -\left(\beta^2+\gamma^2+\dfrac{S_P}{K}\right) \end{pmatrix},$$

$$\mathbf{A}_{\gamma\beta} = \begin{pmatrix} æ+1 & 0 & 0 & 0 \\ 0 & 1 & 0 & 0 \\ 0 & 0 & 1 & 0 \\ 0 & 0 & 0 & 0 \end{pmatrix},$$

$$\mathbf{B}_{\gamma\beta} = \begin{pmatrix} 0 & (3-æ)\beta & (3-æ)\gamma & 0 \\ -\beta & 0 & 0 & 0 \\ -\gamma & 0 & 0 & 0 \\ 0 & 0 & 0 & 1 \end{pmatrix},$$

$$\mathbf{g}_{\gamma\beta} = \begin{pmatrix} (æ-1)(\alpha P_{\gamma\beta} - L_{\gamma\beta}) & Y_{\gamma\beta} & Z_{\gamma\beta} & P_{\gamma\beta} \end{pmatrix}^{\top},$$

$\mathbf{I}$ is a unit matrix.

Appendix B. The subcase of the boundary value vector problem (9) ***when*** $\beta = 0$, $\gamma \neq 0$.

In the case when $\beta = 0$, $\gamma \neq 0$ the boundary value problem (6) transforms to the following form

$$\mathbf{L}_2\mathbf{y}_{\gamma 0}(x) = \mathbf{0}, \qquad 0 < x < \infty,$$

$$\mathbf{A}_{\gamma 0}\mathbf{y}'_{\gamma 0}(0) + \mathbf{B}_{\gamma 0}\mathbf{y}_{\gamma 0}(0) = \mathbf{g}_{\gamma 0}. \qquad \textbf{(B.1)}$$

Here $\mathbf{L}_2\mathbf{y}_{\gamma 0}(x) = \mathbf{I}\mathbf{y}''_{\gamma 0}(x) + \mathbf{Q}_{\gamma 0}\mathbf{y}'_{\gamma 0}(x) + \mathbf{O}_{\gamma 0}\mathbf{y}_{\gamma 0}(x)$, $\mathbf{I}$ is a unit matrix,

$$\mathbf{y}_{\gamma 0}(x) = \begin{pmatrix} u_{\gamma 0}(x) \\ w_{\gamma 0}(x) \\ p_{\gamma 0}(x) \end{pmatrix},$$

$$\mathbf{Q}_{\gamma 0} = \begin{pmatrix} 0 & \dfrac{2\gamma}{æ+1} & -\alpha\dfrac{æ-1}{æ+1} \\ -\dfrac{2\gamma}{æ-1} & 0 & 0 \\ -\dfrac{\alpha}{K} & 0 & 0 \end{pmatrix},$$

$$\mathbf{O}_{\gamma 0} = \begin{pmatrix} -\gamma^2\dfrac{æ-1}{æ+1} & 0 & 0 \\ 0 & -\gamma^2\dfrac{æ+1}{æ-1} & \alpha\gamma \\ 0 & -\dfrac{\alpha\gamma}{K} & -\left(\gamma^2 + \dfrac{S_P}{K}\right) \end{pmatrix},$$

$$\mathbf{A}_{\gamma 0} = \begin{pmatrix} æ+1 & 0 & 0 \\ 0 & 1 & 0 \\ 0 & 0 & 0 \end{pmatrix},$$

$$\mathbf{B}_{\gamma 0} = \begin{pmatrix} 0 & (3-æ)\gamma & 0 \\ -\gamma & 0 & 0 \\ 0 & 0 & 1 \end{pmatrix},$$

$$\mathbf{g}_{\gamma 0} = \begin{pmatrix} (æ-1)(\alpha P_{\gamma 0} - L_{\gamma 0}) & Z_{\gamma 0} & P_{\gamma 0} \end{pmatrix}^{\top}.$$

Analogically to the previous

$$\mathbf{M}_{\gamma 0}(\xi) = \begin{pmatrix} \xi^2 - \gamma^2\dfrac{æ-1}{æ+1} & \dfrac{2\gamma}{æ+1}\xi & -\alpha\xi\dfrac{æ-1}{æ+1} \\ -\dfrac{2\gamma}{æ-1}\xi & \xi^2 - \gamma^2\dfrac{æ+1}{æ-1} & \alpha\gamma \\ -\dfrac{\alpha}{K}\xi & -\dfrac{\alpha\gamma}{K} & \xi^2 - \left(\beta^2 + \dfrac{S_P}{K}\right) \end{pmatrix}.$$

The determinant of the matrix $\mathbf{M}_{\gamma 0}(\xi)$ has two multiple poles of the second order $\xi = \pm\gamma$ and two simple poles

$$\xi = \pm\sqrt{\gamma^2 + \frac{S_P}{K} + \frac{\alpha^2(æ-1)}{K(æ+1)}}.$$

The solution of the boundary value problem **(B.1)** corresponding to the case when $\beta = 0$, $\gamma \neq 0$ has the following form

$$\mathbf{y}_{\gamma 0}(x) = \left(\mathbf{Y}_{\gamma 0,2}(x) + \mathbf{Y}_{\gamma 0,4}(x)\right)\begin{pmatrix} c_{1,1} \\ c_{1,2} \\ c_{1,3} \end{pmatrix}, \qquad \textbf{(B.2)}$$

where constants $c_{1,i}$, $i = 1,2,3$, are found from the boundary conditions in **(B.1)**.

Appendix C. The subcase of the boundary value vector problem (9) ***when*** $\beta \neq 0$, $\gamma = 0$.

In the case when $\beta \neq 0$, $\gamma = 0$ the boundary value problem (6) transforms to the following form

$$\mathbf{L}_2\mathbf{y}_{0\beta}(x) = \mathbf{0}, \qquad 0 < x < \infty,$$

$$\mathbf{A}_{0\beta}\mathbf{y}'_{0\beta}(0) + \mathbf{B}_{0\beta}\mathbf{y}_{0\beta}(0) = \mathbf{g}_{0\beta}. \qquad \textbf{(C.1)}$$

Here $\mathbf{L}_2\mathbf{y}_{0\beta}(x) = \mathbf{I}\mathbf{y}''_{0\beta}(x) + \mathbf{Q}_{0\beta}\mathbf{y}'_{0\beta}(x) + \mathbf{O}_{0\beta}\mathbf{y}_{0\beta}(x)$, $\mathbf{I}$ is a unit matrix,

$$\mathbf{y}_{0\beta}(x) = \begin{pmatrix} u_{0\beta}(x) \\ v_{0\beta}(x) \\ p_{0\beta}(x) \end{pmatrix},$$

$$\mathbf{Q}_{0\beta} = \begin{pmatrix} 0 & \dfrac{2\beta}{æ+1} & -\alpha\dfrac{æ-1}{æ+1} \\ -\dfrac{2\beta}{æ-1} & 0 & 0 \\ -\dfrac{\alpha}{K} & 0 & 0 \end{pmatrix},$$

$$\mathbf{O}_{0\beta} = \begin{pmatrix} -\beta^2\dfrac{æ-1}{æ+1} & 0 & 0 \\ 0 & -\beta^2\dfrac{æ+1}{æ-1} & \alpha\beta \\ 0 & -\dfrac{\alpha\beta}{K} & -\left(\beta^2 + \dfrac{S_P}{K}\right) \end{pmatrix},$$

$$\mathbf{A}_{0\beta} = \begin{pmatrix} æ+1 & 0 & 0 \\ 0 & 1 & 0 \\ 0 & 0 & 0 \end{pmatrix},$$

$$\mathbf{B}_{0\beta} = \begin{pmatrix} 0 & (3-æ)\beta & 0 \\ -\beta & 0 & 0 \\ 0 & 0 & 1 \end{pmatrix},$$

$$\mathbf{g}_{0\beta} = \begin{pmatrix} (æ-1)(\alpha P_{0\beta} - L_{0\beta}) & Y_{0\beta} & P_{0\beta} \end{pmatrix}^{\top}.$$

Analogically to the previous

$$\mathbf{M}_{0\beta}(\xi) = \begin{pmatrix} \xi^2 - \beta^2\dfrac{æ-1}{æ+1} & \dfrac{2\beta}{æ+1}\xi & -\alpha\xi\dfrac{æ-1}{æ+1} \\ -\dfrac{2\beta}{æ-1}\xi & \xi^2 - \beta^2\dfrac{æ+1}{æ-1} & \alpha\beta \\ -\dfrac{\alpha}{K}\xi & -\dfrac{\alpha\beta}{K} & \xi^2 - \left(\beta^2 + \dfrac{S_P}{K}\right) \end{pmatrix}.$$

The determinant of the matrix $\mathbf{M}_{0\beta}(\xi)$ has two multiple poles of the second order $\xi = \pm\beta$ and two simple poles

$$\xi = \pm\sqrt{\beta^2 + \frac{S_P}{K} + \frac{\alpha^2(æ-1)}{K(æ+1)}}.$$

The solution of the boundary value problem **(C.1)** which corresponds to the case when $\beta \neq 0$, $\gamma = 0$ has the following form:

$$\mathbf{y}_{0\beta}(x) = \left(\mathbf{Y}_{0\beta,2}(x) + \mathbf{Y}_{0\beta,4}(x)\right)\begin{pmatrix} c_{2,1} \\ c_{2,2} \\ c_{2,3} \end{pmatrix}, \qquad \textbf{(C.2)}$$

where constants $c_{2,i}$, $i = 1,2,3$, are found from the boundary conditions in **(C.1)**.

Appendix D. The subcase of the boundary value vector problem* (9) *when $\beta = 0$, $\gamma = 0$.

In the case when $\beta = 0$, $\gamma = 0$ the boundary value problem (6) transforms to the following form:

$$\mathbf{L}_2\mathbf{y}_{00}(x) = \mathbf{0}, \qquad 0 < x < \infty,$$

$$\mathbf{B}_{00}\mathbf{y}_{00}(0) = \mathbf{g}_{00}. \qquad \textbf{(D.1)}$$

Here

$$\mathbf{L}_2\mathbf{y}_{00}(x) = \mathbf{J}\mathbf{y}''_{00}(x) + \mathbf{Q}_{00}\mathbf{y}'_{00}(x) + \mathbf{O}_{00}\mathbf{y}_{00}(x), \quad \mathbf{y}_{00}(x) = \begin{pmatrix} u'_{00}(x) \\ p_{00}(x) \end{pmatrix},$$

$$\mathbf{J} = \begin{pmatrix} 0 & 0 \\ 0 & 1 \end{pmatrix}, \qquad \mathbf{Q}_{00} = \begin{pmatrix} 1 & -\alpha\dfrac{æ-1}{æ+1} \\ 0 & 0 \end{pmatrix}, \qquad \mathbf{O}_{00} = \begin{pmatrix} 0 & 0 \\ -\dfrac{\alpha}{K} & -\dfrac{S_P}{K} \end{pmatrix},$$

$$\mathbf{B}_{00} = \begin{pmatrix} 1 & 0 \\ 0 & 1 \end{pmatrix}, \qquad \mathbf{g}_{00} = \left(\frac{æ-1}{æ+1}(\alpha P_{00} - L_{00}) \quad P_{00}\right)^{\top}.$$

Analogically to the previous

$$\mathbf{M}_{00}(\xi) = \begin{pmatrix} \xi & -\alpha\xi\dfrac{æ-1}{æ+1} \\ -\dfrac{\alpha}{K} & \xi^2 - \dfrac{S_P}{K} \end{pmatrix}.$$

The determinant of the matrix $\mathbf{M}_{00}(\xi)$ has one multiple pole of the second order $\xi = 0$ and two simple poles

$$\xi = \pm\sqrt{\frac{S_P}{K} + \frac{\alpha^2(æ-1)}{K(æ+1)}}.$$

The solution of the boundary value problem **(D.1)** which corresponds to the case when $\beta = 0$, $\gamma = 0$ has the following form:

$$\mathbf{y}_{00}(x) = \left(\mathbf{Y}_{00,1}(x) + \mathbf{Y}_{00,3}(x)\right)\begin{pmatrix} c_{0,1} \\ c_{0,2} \end{pmatrix} \qquad \textbf{(D.2)}$$

where constants $c_{0,i}$, $i = 1,2$, are found from the boundary conditions in (**D.1**).

1. *Вайсфельд Н. Д., Журавльова З. Ю.* Плоска змішана задача термопружності для півсмуги // Мат. методи та фіз.-мех. поля. – 2015. – **58**, № 4. – С. 87–98.
   Engl. translation: *Vaisfel'd N. D., Zhuravlova Z. Yu.* Two-dimensional mixed problem of thermoelasticity for a semistrip // J. Math. Sci. – 2018. – **228**, No. 2. – P. 105–121. – https://doi.org/10.1007/s10958-017-3609-8.
2. *Вайсфельд Н. Д., Попов Г. Я.* Смешанная краевая задача теории упругости для четверти пространства // Изв. РАН. Механика твердого тела. – 2009. – № 5. – С. 68–89.
   Engl. translation: *Vaisfeld N. D., Popov G. Y.* Mixed boundary value problem of elasticity for a quarter space // Mech. Solids. – 2009. – **44**, № 5. – P. 712–728. – https://doi.org/10.3103/S0025654409050082.

3. *Гачкевич О. Р., Терлецький Р. Ф., Брухаль М. Б.* Моделювання та дослідження теплового та напруженого станів в опромінюваній системі з шарів різної прозорості, розділених непоглинаючим середовищем // Мат. методи та фіз.-мех. поля. – 2017. – **60,** № 4. – С. 124–136.
   Engl. translation: *Hachkevych O. R., Terletskii R. F., Brukhal' M. B.* Modeling and investigation of thermal and stressed states in an irradiated system of layers with different transparencies separated by nonabsorbing media // J. Math. Sci. – 2020. – **247**, No. 1. – P. 157–172.
   – https://doi.org/10.1007/s10958-020-04794-1.
4. *Кит Г. С., Хай М. В., Лаушник И. П.* Интегральные уравнения трехмерных задач теплопроводности для полупространства с плоскими трещинами // Мат. методы и физ.-мех. поля. – 1984. – Вып. 19. – С. 40–45.
5. *Козачок О. П., Слободян Б. С., Мартиняк Р. М.* Контакт пружного тіла і жорсткої основи з періодичною системою квазіеліптичних виїмок, частково заповнених рідиною, яка змочує поверхні тіл // Мат. методи та фіз.-мех. поля. – 2017. – **60,** № 1. – С. 132–140.
   Engl. translation: *Kozachok O. P., Slobodian B. S., Martynyak R. M.* Contact between an elastic body and a rigid base with periodic array of quasielliptic grooves partially filled with liquid wetting the surfaces of the bodies // J. Math. Sci. – 2019. – **240**, No. 2. – P. 162–172.
   – https://doi.org/10.1007/s10958-019-04344-4.
6. *Кубік Ю., Качмарик М., Чапля Є.* Про методи визначення характеристик пористих насичених середовищ // Фіз.-хім. механіка матеріалів. – 2001. – **37**, № 1. – С. 81–88.
   Engl. translation: *Kubik J., Kachmaryk M., Chaplya E.* Methods for the determination of the characteristics of porous saturated media // Mater. Sci. – 2001. – **37**, No. 1. – P. 92–102. – https://doi.org/10.1023/A:1012342523893.
7. *Кушнір Р. М., Махоркін І. М., Махоркін М. І.* Аналітично-числове визначення статичного термопружного стану плоских багатошарових термочутливих структур // Мат. методи та фіз.-мех. поля. – 2019. – **62,** № 4. – С. 131–140.
   Engl. translation: *Kushnir R. M., Makhorkin I. M., Makhorkin M. I.* Numerical-analytic determination of the static thermoelastic state of plane multilayer thermosensitive structures // J. Math. Sci. – 2022. – **265**, No. 3. – P. 498–511.
   – https://doi.org/10.1007/s10958-022-06067-5.
8. *Попов Г. Я.* Точные решения некоторых краевых задач механики деформируемого твёрдого тела. – Одесса: Астропринт, 2013. – 421 с.
9. *Саврук М. П.* Двумерные задачи упругости для тел с трещинами. – Киев: Наук. думка, 1981. – 324 с.
10. *Станкевич В. З., Михаськів В. В.* Інтенсивність динамічних напружень поздовжнього зсуву у періодично шаруватому композиті з круговими тріщинами // Мат. методи та фіз.-мех. поля. – 2020. – **63**, № 3. – С. 46–54.
    – https://doi.org/10.15407/mmpmf2020.63.3.46-54.
    Engl. translation: *Stankevych V. Z., Mykhas'kiv V. V.* Intensity of dynamic stresses of longitudinal shear in a periodically layered composite with circular cracks // J. Math. Sci. – 2023. – **273**, No. 1. – P. 51–60.
    – https://doi.org/10.1007/s10958-023-06483-1.
11. *Anthony E., Vedanti N.* Simulation of seismic wave propagation in a poroelastic media: an application to a CO_2 sequestration case // 13th Biennial Int. Conf. and Exhibition (Kochi, India, 2020). – 6 p.
    –https://www.researchgate.net/publication/359722486.
12. *Biot M. A.* General theory of three-dimensional consolidation // J. Appl. Phys. – 1941. – **12**, No. 2. – P. 155–164. – https://doi.org/10.1063/1.1712886.
13. *Bociu L., Canic S., Muha B., Webster J. T.* Multilayered poroelasticity interacting with Stokes flow // SIAM J. Math. Anal. – 2021. – **53**, No. 6. – P. 6243–6279.
    – https://doi.org/10.1137/20M1382520.
14. *Castro A. P. G., Yao J., Battisti T., Lacroix D.* Poroelastic modeling of highly hydrated collagen hydrogels: experimental results vs. numerical simulation with custom and commercial finite element solvers // Front. Bioeng. Biotechnol. Sec. Biomech. – 2018. – **6**. – Article 142. – 8 p. – https://doi.org/10.3389/fbioe.2018.00142.
15. *Cheng A. H.-D.* Poroelasticity. – Cham: Springer, 2016. – xxvi+877 p. – Ser. Title: Theory and Applications of Transport in Porous Media. – Vol. 27.
    – https://doi.org/10.1007/978-3-030-64308-9_3.
16. *Dong H., Kaynia A. M., Madshus Ch., Hovem J. M.* Sound propagation over layered

poro-elastic ground using a finite-difference model // J. Acoust. Soc. Am. – 2000. – **108**, No. 2. – P. 494–502. – https://doi.org/10.1121/1.429579.
17. *Gantmacher F. R.* The theory of matrices. – New York: Chelsea Publ. Co., 1959. – Vol. 1: x+374 p.; Vol. 2: x+277 p.
18. *Gilbert R. P., Lee D.-S., Ou M.-J. Y.* Lamb waves in a poroelastic plate // J. Comput. Acoust. – 2013. – **21**, No. 02. – Article 1350001. – 25 p. – https://doi.org/10.1142/S0218396X1350001X.
19. *Jin B.* Dynamic displacements of an infinite beam on a poroelastic half space due to a moving oscillating load // Arch. Appl. Mech. – 2004. – **74**, No. 3-4. – P. 277–287. – https://doi.org/10.1007/BF02637202.
20. *Keawsawasvong S., Senjuntichai T.* Dynamic interaction between elastic plate and transversely isotropic poroelastic medium // MATEC Web Conf., SCESCM 2018. – 2019. – **258**. – Article 05016. – https://doi.org/10.1051/matecconf/201925805016.
21. *Li J., Ostoja-Starzewski M.* Thermo-poromechanics of fractal media // Phil. Trans. R. Soc. **A**. – 2020. – **378**, No. 2172. – Article 20190288. – https://doi.org/10.1098/rsta.2019.0288.
22. *Liu J., Cui Zh., Sevostianov I.* Effect of stresses on wave propagation in fluid-saturated porous media // Int. J. Eng. Sci. – 2021. – **167**. – Article 103519. – https://doi.org/10.1016/j.ijengsci.2021.103519.
23. *Lucantonio A., Tomassetti G., DeSimone A.* Large-strain poroelastic plate theory for polymer gels with applications to swelling-induced morphing of composite plates // Compos. **B**: Eng. – 2017. – **115**. – P. 330-340. – https://doi.org/10.1016/j.compositesb.2016.09.063.
24. *Nahirnyj T., Tchervinka K.* Mathematical modeling of the coupled processes in nanoporous bodies // Acta Mech. Automat. – 2018. – **12**, No. 3. – P. 196–203. – https://doi.org/10.2478/ama-2018-0030.
25. *Pimenta C., Wolf W. R., Cavalieri A. V. G.* A fast numerical framework to compute acoustic scattering by poroelastic plates of arbitrary geometry // J. Comput. Phys. – 2018. – **373**. – P. 763–783. – https://doi.org/10.1016/j.jcp.2018.07.019.
26. *Rauch A. D., Vuong Anh-Tu, Yoshihara L., Wall W. A.* A coupled approach for fluid saturated poroelastic media and immersed solids for modeling cell-tissue interactions // Int. J. Num. Meth. Biomed. Eng. – 2018. – **34**, No. 11. – e3139. – https://doi.org/10.1002/cnm.3139.
27. *Reddy P. M., Tajuddin M.* Edge waves in poroelastic plate under plane stress conditions // J. Acoust. Soc. Am. – 2003. – **114**, No. 1. – P. 185–193. – https://doi.org/10.1121/1.1569258.
28. *Rudnicki J. W.* Linear poroelasticity // Handbook of materials behavior models: Three-Volume Set: Nonlinear models and properties / J. Lemaitre (Ed.). – Vol. III. – San Diego etc.: Acad. Press, 2001. – Sec. 11.6. – P. 1118–1125. – https://doi.org/10.1016/B978-012443341-0/50113-7.
29. *Shah S. A., Tajuddin M.* Three dimensional vibration analysis of an infinite poroelastic plate immersed in an inviscid elastic fluid // Int. J. Eng. Sci. Tech. – 2011. – **3**, No. 2. – P. 1–11. – https://doi.org/10.4314/ijest.v3i2.68127.
30. *Smith J. D., Heimisson E. R., Bourne S. J., Avouac J.-Ph.* Stress-based forecasting of induced seismicity with instantaneous earthquake failure functions: Applications to the Groningen gas reservoir // Earth Planet. Sci. Lett. – 2022. – **594.** – Article 117697. – https://doi.org/10.1016/j.epsl.2022.117697.
31. *Smith M. J. A., Peter M. A., Abrahams I. D., Meylan M. H.* On the Wiener – Hopf solution of water-wave interaction with a submerged elastic or poroelastic plate // Proc. R. Soc. **A**. – 2020. – **476**, No. 2242. – Article 20200360. – https://doi.org/10.1098/rspa.2020.0360.
32. *Tan W. S., Moore A. C., Stevens M. M.* Minimum design requirements for a poroelastic mimic of articular cartilage // J. Mech. Behavior Biomed. Mater. – 2023. – **137**. – Article 105528. – https://doi.org/10.1016/j.jmbbm.2022.105528.
33. *Theodorakopoulos D. D.* Dynamic response of poroelastic plates // Trans. Built Environ. – 1993. – **3**. – P. 275–289.
34. *Vaysfeld N. D., Zhuravlova Z. Yu.* Response of a poroelastic semi-infinite strip to the compression acting upon its lateral sides // Мат. методи та фіз.-мех. поля. – 2022. – **65**, № 1-2. – P. 199–208.
35. *Verruijt A.* An introduction to soil dynamics. – Dordrecht: Springer, 2010. – xiv+433 p. – Ser.: Theory and applications of transport in porous media. – Vol. 24.
36. *Wang Sh., Li S., Wu Y.-Sh.* An analytical solution of pressure and displacement induced by recovery of poroelastic reservoirs and its applications // Soc. Petrol. Eng.

J. (SPE J.) – 2023. – **28**, No. 3. – Paper Number: SPE-214290-PA. – P. 1329–1348. – https://doi.org/10.2118/214290-PA.
37. *Wheatley B. B., Odegard G. M., Kaufman K. R., Donahue T. L. H.* A case for poroelasticity in skeletal muscle finite element analysis: experiment and modeling // Comput. Meth. Biomech. Biomed. Eng. – 2017. – **20**, No. 6. – P. 598–601. – https://doi.org/10.1080/10255842.2016.1268132.
38. *Yang J., Sato T.* Dynamic response of saturated layered half-space with different hydraulic interface conditions // Arch. Appl. Mech. – 1998. – **68**, No. 10. – P. 677–688. – https://doi.org/10.1007/s004190050196.
39. *Yuzvyak M., Tokovyy Yu.* Thermal stresses in an elastic parallelepiped // J. Therm. Stress. – 2022. – **45**, No. 12. – P. 1009–1028. – https://doi.org/10.1080/01495739.2022.2120940.
40. *Zhuravlova Z.* Exact solution of the plane problems for poroelastic rectangle and semi-strip // Z. Angew. Math. Mech. – 2022. – **102**, No. 11. – e202200162. – https://doi.org/10.1002/zamm.202200162.

МЕХАНІЧНИЙ ПОРОПРУЖНИЙ ВІДГУК НАПІВНЕСКІНЧЕННОГО КУБОЇДА НА ЗОВНІШНЄ НАВАНТАЖЕННЯ

Новизна запропонованої роботи полягає в отриманні точного аналітичного розв'язку тривимірної задачі поропружності для напівнескінченного кубоїда. Розв'язування тривимірних задач поропружності зумовлює значні математичні труднощі через розмірність системи диференціальних рівнянь, яку потрібно розв'язати. Традиційно такі розв'язки отримують переважно за допомогою різних числових підходів. Запропоновану задачу сформульовано як тривимірну крайову задачу в термінах моделі Біо, що розглядає повністю зв'язану поведінку гомогенізованої фази твердого тіла, що базується на структурному каркасі, та гомогенізованої фази рідини, що описує взаємопроникну рідину. Для отримання розв'язку застосовано аналітичний метод інтегральних перетворень. Це дозволило отримати явні вирази, що описують напруження у твердому каркасі та тиск рідини у порах. Проведено дослідження залежності цих характеристик від різних поропружних властивостей матеріалу та типу прикладеного навантаження. Отримані числові результати можуть бути використані в інженерному моделюванні поропружних структур, а також як еталонні при розробці нових числових методів розв'язання задач тривимірної поропружності.

Ключові слова: *поропружний напівнескінченний кубоїд, інтегральне перетворення, матричне диференціальне числення, точний розв'язок.*

Odesa I. I. Mechnikov National University, Odesa

Received
22.04.23